Distributed Stress Measurement in Steel Plates Based on Remnant Magnetization and Magnetoelastic Effect

Hongbin Zhang, Yuan Wang, Qian Chen, Jinyu Ma, Jian Li, and Xinjing Huang

***Abstract*— In this article, we propose a highly consistent and sensitive method for steel plate stress measurement based on strong remnant magnetization and magnetoelastic effect. Firstly, the J-A force-magnetic coupling model is theoretically improved, and the influencing factors of the force-magnetic coupling strength are investigated via parameter sweeping, and it is determined that the magnetization can reduce the initial permeability to improve the sensitivity and consistency of the stress measurement. Then the equation of the coil electromagnetic impedance change in the magnetic circuit versus the stress is deduced, and it is obtained that the stress has a negative linear relationship with the coil impedance, and the sensitivity increases with the increase of the excitation frequency, which is verified by the single-point stress measurement experiment of the sandwich steel plates. Finally, the distributed stress measurement experiments of sandwich steel plates are carried out, which proved that the impedance values at different measurement points after the steel plates are magnetized can successfully reflect the distribution state of the stress. After magnetization, the stress measurement sensitivity of the electromagnetic impedance method increases on average from 0.014 Ω/MPa before magnetization to 0.037 Ω/MPa, with an enhancement of 2.6×. The measurement accuracy under different loads increases on average from 50.699 MPa before magnetization to 7.078 MPa, with an enhancement of 7.2×.**

***Index Terms*— Magnetization, magnetoelasticity, steel, stress measurement.**

I. Introduction

FERROMAGNETIC materials are widely used in steel components [1], pressure vessels [2], bridges [3], oil and gas transportation pipelines [4], and other large-scale equipment due to their high strength, high-temperature resistance, corrosion resistance, and good toughness. With the increase of service time, corrosion or external damage will lead to the redistribution of stress in ferromagnetic components, forming local stress concentrations, and in serious cases, fracture will occur, causing serious safety accidents; therefore, the pre-stress testing of ferromagnetic materials is important to judge the safety of the structure.

Currently, the commonly used stress measurement methods are based on strain meter, acoustoelastic effect, or magnetoelastic effect. The strain meter method requires attaching resistance strain meters or fiber Bragg gratings (FBGs) on the surface of the part under test and calculates the stress by detecting the surface strain, which can only realize the stress monitoring of a limited number of fixed points. For beams with analytical expressions of deflection, the spatially discrete sampled values of stresses can be fit using the deflection equations of the beams to realize distributed stress measurements [5], [6]. Whereas, for structures with complex support conditions or huge dimensions, such as buried pipelines and railroad tracks, the deflection equations cannot be obtained beforehand, and movable measurement instead of fixed measurement is more practical.

The speed of ultrasound propagation in a material varies linearly with the material stress, and the acoustic elasticity method uses this property to achieve stress measurement in materials. According to the ultrasonic modes, the acoustic elasticity method is categorized into longitudinal wave, shear wave, and critical refracted longitudinal wave methods [7], [8]. The acoustic elasticity method requires the application of a coupling agent on the contact surface of ferromagnetic components and the sensors and has high requirements for the installation accuracy of the module, which is suitable for localized stress measurement of ferromagnetic components in the laboratory environment and is not conducive to on-site stress measurement.

According to whether an external excitation magnetic field is applied or not, the methods of stress measurement based on the magnetoelastic effect can be divided into two types: active magnetization and passive magnetization. Passive magnetization is also known as the magnetic memory method. When ferromagnetic parts are machined, the combined effect of the load and the geomagnetic field causes an irreversible reorientation of the magnetic domain organization in the stress concentration region of the part, and this change is maintained even after the load is removed, and the magnetic anomalies on the surface "remember" the location of the stress concentration [9]. Ren and Ren [10] confirmed that the magnetic field and

Manuscript received 2 August 2023; revised 4 October 2023; accepted 5 October 2023. Date of publication 19 October 2023; date of current version 1 November 2023. This work was supported in part by the National Nature Science Foundation of China under Grant 62073233 and in part by the Natural Science Foundation of Tianjin under Grant 21JCQNJC00690. The Associate Editor coordinating the review process was Dr. Hamed Hamzehbahmani. *(Hongbin Zhang and Yuan Wang contributed equally to this work.) (Corresponding author: Xinjing Huang.)*

Hongbin Zhang, Yuan Wang, and Qian Chen are with the College of Precision Instrument and Opto-Electronics Engineering, Tianjin University, Tianjin 300072, China.

Jinyu Ma, Jian Li, and Xinjing Huang are with the State Key Laboratory of Precision Measurement Technology and Instruments, Tianjin University, Tianjin 300072, China (e-mail: huangxinjing@tju.edu.cn).

Digital Object Identifier 10.1109/TIM.2023.3325525

the stress at the stress concentration are linearly related under certain magnitude of stress conditions by repeated loading and unloading experiments on steel plates. Qiu et al. [11] found that the redistribution of spin reorientation and orbital coupling induced by strain in ferromagnetic materials is responsible for changing the magnetic field of ferromagnetic materials. Li et al. [12] conducted a study on the sensitivity of stress-concentrated magnetic measurement and concluded that the use of a force-magnetic coupling model can effectively predict the magnetization law under the applied stress and qualitatively describe the pattern of change of magnetic induction on the surface. Because of the different historical effects, the specimen often has a different initial state of magnetization and cannot obtain a consistent initial amplitude, which makes it difficult to quantify the relationship between the surface magnetic field and the stress, the force-magnetic measurement signal is low in sensitivity, and it does not meet the requirements of the field application [12], [13].

Active magnetization mainly consists of the magnetic Barkhausen noise (MBN) method and the magnetic anisotropy method. The MBN method uses an excitation coil to magnetize a ferromagnetic material with a gradual intensity to change its magnetic domain distribution and uses a receiving coil to pick up the electromagnetic noise signal generated by the movement of the magnetic domains inside the ferromagnetic material to analyze the stress distribution [14]. Liu et al. [15] used a hybrid magnetic sensing mode to measure stress in ferromagnetic materials and designed a hybrid magnetic sensing structure for measuring eddy currents, alternating electromagnetic fields, MBN, and incremental permeability signals; the stress detection validation test was also performed on oriented silicon steel samples. Qiu et al. [16] investigated the magnetic domain dynamics and the MBN values of grain-oriented transverse and longitudinal electrical steels using time-resolved magneto-optical imaging and studied the time-domain and frequency-domain characteristics of the MBN signals to assess the stress state and magneto crystalline anisotropy. The complex process of magnetic domain alignment in transverse electrical steels was revealed by magnetic domain imaging, providing physical insight into bulk micromagnetic phenomena. The MBN method is more effective in detecting localized stresses in fixed points and is less used on large parts for which mobile stress measurement is required.

The magnetic anisotropy method determines the direction and magnitude of stress by applying a weak ac magnetization to the test piece and detecting the change in permeability of the material in different directions. Doi et al. [17] illustrated the relationship between the stress tensor and the magnetization vector; simulation results show that the magnetic anisotropy exhibited by the different flux density distributions of ferromagnetic materials can reflect the different stress distributions of ferromagnetic materials. Zhang et al. [18] developed a model for unidirectional stress-induced anisotropy of the magnetic permeability of materials. By conducting loading and unloading experiments on steel plates, it was confirmed that the magnetic induction strength near the material surface can be used to quantitatively assess the magnitude of the stress. Xin et al. [19] established the equivalent magnetic circuit of a nine-pole magnetic measurement probe, analyzed the influence of parameters such as the number of turns of the probe coil and the current size on the effect of stress measurement in ferromagnetic materials, and confirmed that the nine-pole probe can effectively measure the residual stress of ferromagnetic materials. Su et al. [20] proposed a method for detecting stress concentration in pipelines based on unsaturated magnetization, analyzed the effects of excitation source position, sensor lift-off value, and stress concentration value on the response signal, and confirmed that the axial magnetic component can better characterize the stress concentration. Tong et al. [21] measured the magnetic field on the surface of the steel bar under tensile load in the geomagnetic environment by using a triaxial magnetometer and estimated the stress change according to the J-A model; however, due to the weak geomagnetic field, it is not enough to make the magnetic domain overcome the friction to achieve the same direction, so the consistency and sensitivity of the magnetic measurement are poor.

In this article, a stress measurement method for ferromagnetic steel plates based on strong remnant magnetization and magnetoelastic effect is proposed. First, the relationship between the permeability of ferromagnetic materials and the applied stress, as well as its influencing factors, are analyzed according to the J-A model, and the mechanism of strong remnant magnetization to enhance the coupling sensitivity of the stress and the permeability is clarified. Then, the expression of the linear relationship between the stress and the electromagnetic impedance change of the coil detector is deduced when the tested parts are connected in series with the ac detection coils to form a magnetic circuit. Finally, an experimental setup of a sandwich structure that can generate uniform stress is built to experimentally verify the relationship between distributed stresses and impedances on steel plates and demonstrate that strong magnetization enables successful measurement of stress distribution.

II. Measurement Principle

A. Effects of Magnetization on $\boldsymbol{\mu_r}(\boldsymbol{\sigma})$

According to the J-A model, the change in magnetization intensity due to stress changes in ferromagnetic materials can be equated to the magnetization of an equivalent magnetic field H_σ [22], [23], whose expression is given in

$$H_\sigma = \frac{3}{2}\frac{\sigma}{\mu_0}\left(\frac{d\lambda}{dM}\right)_\sigma \tag{1}$$

where σ is the stress of the ferromagnetic material, μ_0 is the permeability of vacuum, λ is the magnetostrictive coefficient, which depends on the magnetic domain structure of ferromagnetic materials, and M is the magnetization strength of the material. For polycrystalline ferromagnetic materials with disordered orientation, the factors affecting the magnetostriction coefficient are complex and are usually represented by the Taylor series in

$$\lambda = \sum \gamma_i(\sigma) M^{2i}. \tag{2}$$

$\gamma_i(\sigma)$ is expanded into (3) using the Taylor series

$$\gamma_i(\sigma) = \gamma_i(0) + \sum \frac{\sigma^n}{n!}\gamma_i^n(0) \tag{3}$$

where $\gamma_i^n(0)$ is the nth order derivative of γ_i when $\sigma = 0$. For the convenience of calculation, taking $i = 2$ and $n = 2$, we can obtain

$$H_\sigma = \frac{3\sigma}{\mu_0\mu_{r0}}\left[\left(\gamma_1(0) + \gamma_1'(0)\sigma\right)M + 2 * \left(\gamma_2(0) + \gamma_2'(0)\sigma\right)M^3\right]. \tag{4}$$

The nonhysteretic magnetization M_{an} of ferromagnetic material under stress is given by the Langevin equation as shown in

$$M_{an}(H,\sigma) = M_s\left[\coth\left(\frac{H + H_\sigma + \alpha M}{b} - \frac{b}{H + H_\sigma + \alpha M}\right)\right] \tag{5}$$

where H is the external magnetic field, $b = (k_B T)/(\mu_0 M)$ is the material constant, α is the magnetic domain coupling coefficient, k_B is the Boltzmann's constant, and M_s is the saturation magnetization strength. According to the proximity principle [24], the derivative of the intensity of the irreversible magnetization is proportional to the change in the irreversible component of the hysteresis-free magnetization. Combining the definitions of magnetoelastic energy and relative permeability, the stress σ as a function of the material's magnetization M and relative permeability μ_r is given in

$$\frac{d\mu_r}{d\sigma} = \frac{\sigma}{H\varepsilon^2}(M_{an} - M) + \frac{c}{H}\frac{dM_{an}}{d\sigma} \tag{6}$$

when σ is 0, μ_r takes the initial value of μ_{r0}. c is the ratio of the initial magnetization rate to the initial hysteresis-free magnetization rate. $\varepsilon^2 = E\xi$, where E is the elastic modulus of material and ξ is the attenuation coefficient associated with the energy per unit volume. In (6), the stress values solved by the differential equation for magnetic permeability are affected by M_{an} and μ_{r0}. According to (5), it can be seen that M_{an} is affected by b, c, α and H. The effects of the different parameters mentioned above on μ_r-σ are analyzed via numerical calculations and the results are shown in Fig. 1. The initial values of μ_0, M_s, ξ, E, γ_1', γ_2', γ_1, and γ_2 are equal to $4\pi \times 10^7$ N/A^2, 1.71×10^6 A/m, 609Pa, 200GPa, -1×10^{-26} A^{-2}Nm, -5×10^{-39} A^{-2}Nm, 2×10^{-18} A^{-2}m^2, and 2×10^{-30} A^{-2}m^2 respectively.

As shown in Fig. 1, the shapes of the μ_r-σ curves are basically similar for different parameters. As the tensile (compressive) stress $|\sigma|$ to which the material is subjected gradually increases, μ_r will first increase and then decrease. The local maximum value of μ_r is obtained at -80 and 121 MPa, respectively. Within the two extremes, μ_r and σ are approximately linear. From Fig. 1(a), (d), and (e), it can be seen that decreasing the material constant b and the initial relative permeability μ_{r0}, or increasing the magnetic domain coupling coefficients α can all increase the slopes of the curves in the interval of the two extreme points of the μ_r-σ curve, and subsequently improve stress detection sensitivity. From Fig. 1(b) and (c), it can be seen that the ratio of the initial magnetization rate to the initial hysteresis-free magnetization rate c, and the external magnetic field H, have a small effect on the μ_r-σ curves, as well as the stress sensitivity.

The mechanism of influence of each parameter is further analyzed. The material constant b decreases as the magnetization M increases. The magnetic domain coupling coefficient α indicates the coupling strength of each magnetic moment of the material with M, and the two coupling directions are the same, which can increase the value of α. Saturated magnetization can reduce the initial relative permeability of the material μ_{r0}; therefore, it is possible to increase the residual magnetization of the material by strong magnetization, which, in turn, decreases the values of b and μ_{r0} and increases the value of α, ultimately increasing the sensitivity of the stress measurement. At the same time, strong magnetization can make the residual magnetization strength of the material more uniform and consistent, improving the consistency of stress measurement. The effect of each parameter on the sensitivity of the force-magnetic coupling is summarized in Fig. 2.

B. Electromagnetic Impedance Method of Stress Measurement

As shown in Fig. 3(a), the ferromagnetic material is connected in series with the core of the ac excitation coil to form a closed magnetic circuit. When the stress in the ferromagnetic material changes, the relative permeability of the material in the magnetic circuit, the magnetic flux, and the coil impedance will change; therefore, the change in relative permeability of the ferromagnetic material and the change in stress can be determined from the change in coil impedance.

According to [25], the relationship between the initial permeability μ_s and the permeability μ_σ under the stress σ is given by the following equation:

$$\frac{\mu_\sigma - \mu_s}{\mu_s} = -2\lambda_s\sigma\mu_s/B_s^2 \tag{7}$$

where B_s is the saturation magnetic induction intensity, λ_s is the saturation magnetostriction coefficient, and σ is the stress. A weak sinusoidal current signal $i = I\sin(\omega t)$ passes through the coil. When the stress on the steel plate is changed, its magnetoresistance changes. The change in the flux of the excitation coil, $\Delta\phi_i$, and the change in the induced voltage, Δu_s, can be expressed as follows:

$$\Delta\phi_i = \frac{N_e i}{R_m + R_{s\sigma}} - \frac{N_e i}{R_m + R_s} \tag{8a}$$

$$\Delta u_s = N_e\frac{d\Delta\phi_i}{dt} = \frac{N_e^2 I\omega\cos(\omega t)}{(R_s + 2R_m)R_s}(R_s - R_{s\sigma}) \tag{8b}$$

wherein ω is the angular frequency, t is the time, N_e is the number of turns of the excitation coil, R_m is the magnetoresistance of the magnetic core, $R_s = l/S\mu_s$ is the initial reluctance of the tube wall, μ_s is the initial permeability, l is the length of the magnetic circuit, S is the flux cross-sectional area, and $R_{s\sigma} = l/S\mu_\sigma$ is the magnetoresistance after the steel plate's stress varies. The coil resistance is small compared to the inductive reactance, so the change in coil impedance is approximately equal to the change in coil inductive reactance.

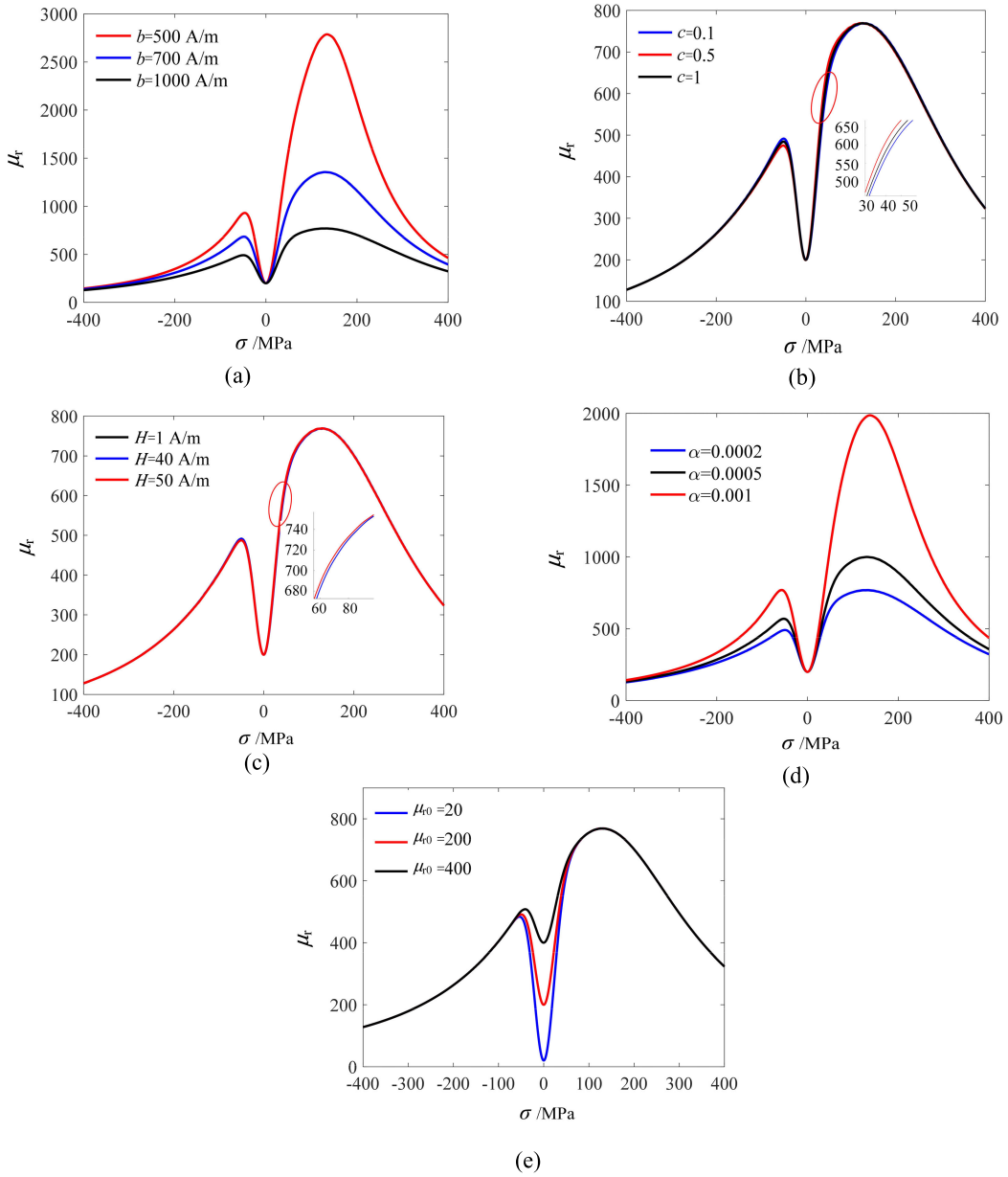

Fig. 1. μ_r-σ curves corresponding to different parameters. (a) Sweeping material constant b. ($c = 0.1$, $H = 40$ A/m, $\alpha = 0.0002$, $\mu_{r0} = 200$, $\alpha = 0.0002$). (b) Sweeping the ratio of initial susceptibility to initial nonhysteresis susceptibility c. ($b = 1000$ A/m, $H = 40$ A/m, $\alpha = 0.0002$, $\mu_{r0} = 200$). (c) Sweeping external magnetic field H. ($b = 1000$ A/m, $c = 0.1$, $\alpha = 0.0002$, $\mu_{r0} = 200$). (d) Sweeping magnetic domain coupling coefficient α. ($b = 1000$ A/m, $c = 0.1$, $H = 40$ A/m, $\mu_{r0} = 200$). (e) Sweeping initial relative permeability μ_{r0}. ($b = 1000$ A/m, $c = 0.1$, $\alpha = 0.0002$, $H = 40$ A/m).

The change in impedance can be expressed as follows:

$$\Delta|Z| \approx \omega \Delta L_s = -\omega \left| \frac{\Delta u_s}{di/dt} \right| = \frac{N_e^2 \omega {\mu_s}^2 S}{l} \frac{2\lambda_s \sigma}{B_s^2 - 2\lambda_s \sigma \mu_s} \tag{9}$$

where l is the length of the magnetic circuit, and S is the flux cross-sectional area. B_s, $|\lambda_s|$, $|\sigma|$, and μ_s take values in the range of 0.5–1 T, 1×10^{-7}–1×10^{-8}, 0–5×10^7 Pa and 2.5×10^{-4}–5×10^{-4} H/m, respectively. Since $B_s \gg 2\lambda_s \sigma \mu_s$, (9) can, therefore, be simplified as follows:

$$\Delta|Z| = -\frac{N_e^2 \omega \mu_s^2 S}{l} \frac{2\lambda_s \sigma}{B_s^2} = -k\sigma \tag{10}$$

where k is a positive number and is related to parameters such as the number of turns of the coil, the flux area, and the magnitude and frequency of the excitation current. From (10), it can be seen that there is a negative linear relationship between coil impedance Z and stress, and the sensitivity is in direct proportion to the excitation frequency.

III. Experiment

A. Stress Generation Method

An experimental device with a sandwich structure, as shown in Fig. 4, is designed to simulate the stress state of steel plates. FBGs are used to measure the strains as references at different locations of the steel surface under different loads. The size of the upper and lower steel plates of the designed sandwich structure is $3000 \times 120 \times 3$ mm, and the material is Q235. Q235 has a Young's modulus of 210 GPa, a Poisson's ratio of 0.3, and a density of 7.85 g/cm^3. In order to ensure that

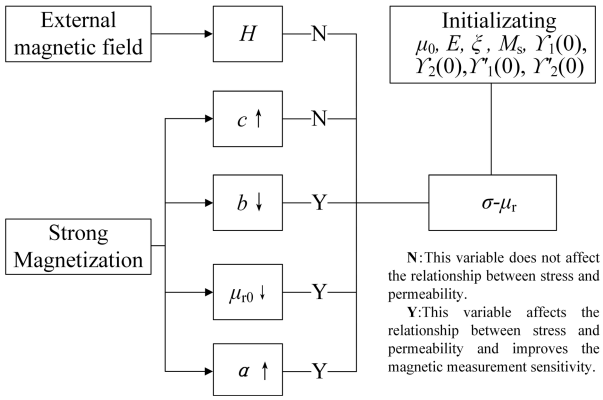

Fig. 2. Schematic of the influence of magnetization on the parameters of the force-magnetic coupling model.

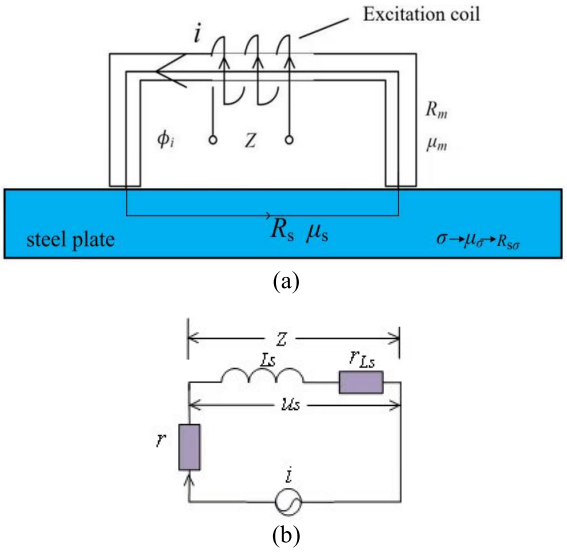

Fig. 3. Principle of stress measurement by electromagnetic impedance method. (a) Magnetic flux path. (b) Equivalent circuit.

the surface of the upper and lower steel plates is farther away and reduce the stress concentration of the intermediate support points, a neutral layer with a size of 3000 × 120 × 20 mm is added in the middle, and the material is PA6, which has a Young's modulus of 2 GPa and a density of 1.13 g/cm^3. Standard weights of W = 0, W = 1, W = 2, W = 3, W = 4, and W = 5 kg are placed at the two ends of the steel plate to make the plate bend to different extents, and the stress values at different locations are measured. The upper steel plate is in tension when a downward bending load is applied to the plate. In the experiment, the upper and lower steel plates are fixed with ties together with the central plastic block, and the electromagnetic probe is fixed in the central area of the upper plate to measure the stresses under different loads. The electromagnetic probe can move on the plate surface.

Ideally, the stress distribution in the sandwich structure is uniform, and there is no sudden change in stress. The stress in the upper steel plate is proportional to its deformation, so a polynomial function is considered to fit the measured stress at different locations. After comparison, the sixth-order polynomial function is finally selected for fitting. The stress

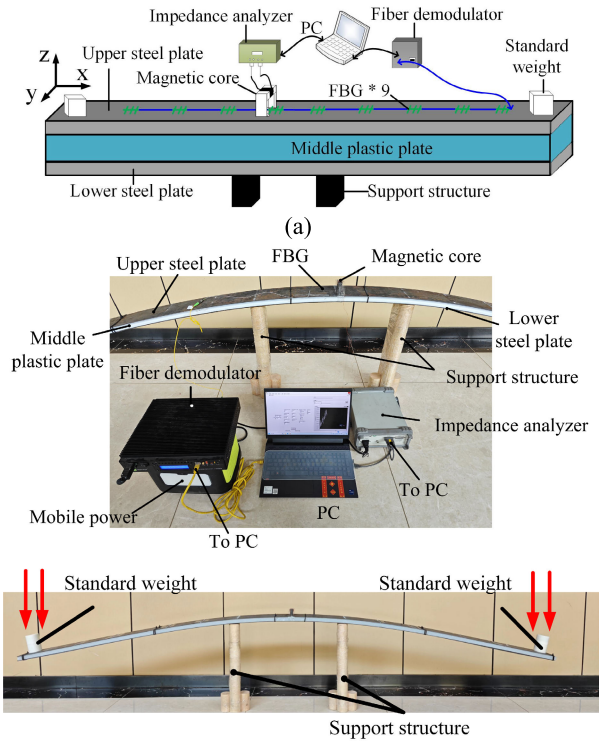

Fig. 4. Stress loading and measurement apparatus. (a) Schematic. (b) Apparatus picture.

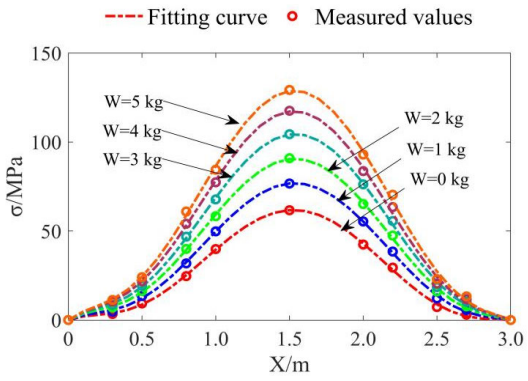

Fig. 5. Stress measured by FBGs at different points on the plate under different loads and the fitting results.

scatter plots at different locations of the sandwich structure are plotted and fit to obtain the fit curves, as shown in Fig. 5.

As can be seen from Fig. 5, the stresses in different regions increase correspondingly with increasing load, and the stress distribution is symmetrical about the center of the steel plate. The true stress values of the experimental steel plates at any point are then obtained from the fit curves.

B. Probe Configuration

The probe is composed of a ferrite core and an excitation coil. The ferrite core is wound by the excitation coil, and an impedance analyzer is used to apply an ac signal to the excitation coils, thereby generating an induced magnetic field that causes eddy currents inside the steel plate. As the stress on the surface of the steel plate changes, so does the magnetic field generated by the eddy currents themselves,

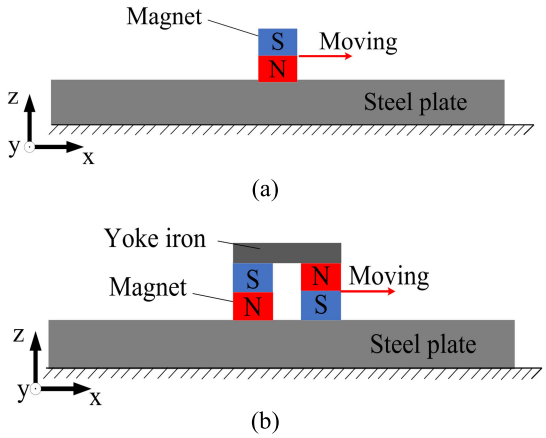

Fig. 6. Methods of magnetizing the steel plate with magnets. (a) Single magnet magnetizes the steel plate. (b) Dual magnet magnetizes the steel plate.

which can change the magnetic flux through the excitation coil and cause a change in the coil impedance that can be read by the impedance analyzer. The excitation coil can generate an excitation magnetic field and form a magnetic flux loop with the magnetic core and the steel plate to be tested. Soft magnetic ferrite with high permeability and high maximum permeability can be used as a probe ferrite core. In this article, based on the selected probe size, the wire diameter of the excitation coil is selected to be $d = 0.17$ mm, the material is brass enameled wire, and the number of turns of the coil is 110.

C. Magnetization Scheme

Inconsistent initial magnetization strength of ferromagnetic specimens may lead to a low signal-to-noise ratio and poor consistency in stress measurement by magnetic methods. One of the solutions to this problem is to magnetize the samples in advance and make them uniformly magnetized. In an earlier study, our laboratory investigated the distribution of residual magnetization strength and residual flux density of steel plates after magnetization by moving single and dual magnets. The model of a magnetized steel plate with magnets is shown in Fig. 6.

When the magnet is placed on top of the steel plate, the magnet generates a stable spatial magnetic field. This spatial magnetic field changes the internal magnetization strength of the steel plate so that the magnetization distribution inside the steel plate is consistent with the magnitude and direction of the external magnetic field. When the magnet moves above the steel plate, it corresponds to a stable magnetic field moving in parallel, and for a fixed point on the surface of the steel plate, the external field decreases from the maximum field to zero.

According to our previous research results [26], the remanence of ordinary steel plates is relatively weak, and the steel plates can be uniformly magnetized by either single magnet or double magnets, and the magnetization effect is the same. This conclusion can be demonstrated by the experimental results in [26] that the magnetic flux density curves near the surface of the steel plate with single-magnet and double-flipping-magnet magnetizations almost overlap. For ordinary steel plates, both single magnet and double magnets can make the residual magnetization intensity of the steel plate become uniform. In our following experiment, the sandwich structure is placed flat on the ground, and the single magnet is moved slowly and uniformly along the x-axis direction on the upper steel plate to magnetize it.

It is, however, possible that the remanence of some steel under test is stronger than what can be produced by a single magnet, and uniform magnetization cannot be achieved using a single magnet. For this exception, we can increase the number of magnets in a single magnet group or use a pair of flipping magnets to form a magnetization loop to enhance the magnetization ability.

TABLE I
COMPARISON OF STRESS MEASUREMENT PERFORMANCE BEFORE AND AFTER MAGNETIZATION

Index	Without magnetization	With magnetization
$\|k\|$/(Ω/MPa)	0.014	0.018
RMSE/Ω	0.076	0.059
RMSE/$\|k\|$ /(MPa)	5.429	3.278

IV. Result and Analysis

A. Single Point Stress Measurement

Frequency sweeping tests of single point stress measurement were carried out with and without magnetization applied to the sandwich structure. The sandwich structure was placed flat on the ground and standard weights of W = 0, W = 1, W = 2, W = 3, W = 4, W = 5 kg were loaded at each end of the sandwich structure. The excitation frequencies were set to 1, 2, 5, 10, 12, 14, 17, 19, 20, 25, and 30 kHz, respectively. The impedance values measured by the probe at the center of the steel plate versus the stress values measured by the FBG were plotted and shown in Fig. 7. It can be seen from Fig. 7 that no matter whether the sandwich structure is magnetized or not when the stress variation is consistent, the impedance variation increases with the increase of the excitation frequency. Magnetization can increase the linearity of ΔZ-σ. In order to achieve high sensitivity, the excitation frequency is set to 30 kHz in the subsequent stress test experiments.

In order to evaluate the sensitivity quantitatively, linear fitting and fitting parameter analysis was carried out on the measured impedance variance ΔZ and stress variance σ under different load conditions at 30 kHz. The results with and without magnetization are shown in Fig. 8 and Table I. It can be seen that the impedance Z decreases as the loading stress σ increases, while magnetization increases the linearity between the coil impedance variance ΔZ and the loading stress σ. The goodness of fitting R^2 before magnetization is 0.9872, while the goodness of fit R^2 after magnetization is 0.9952. It can also be seen from Fig. 8 that magnetization increases the slope of the fit curve, i.e., the sensitivity is enhanced by magnetization.

The root mean square error (RMSE) is used to measure the deviation fluctuation of the stress measurement. The smaller the RMSE value, the better the stability of the measurement.

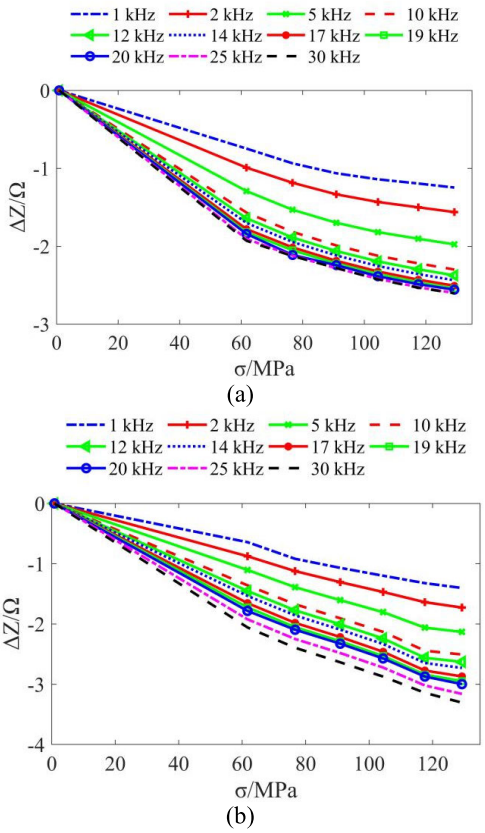

Fig. 7. Frequency sweeping test results. (a) Without magnetization. (b) With magnetization.

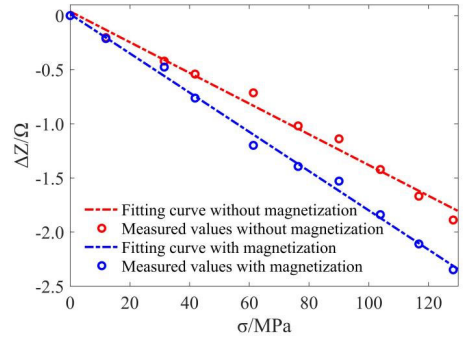

Fig. 8. ΔZ-σ curve at one fixed point when f is 30 kHz.

The absolute value of the slope of the linear fit $|k|$ provides a measure of the impedance-stress measurement sensitivity. After magnetization, $|k|$ becomes larger, indicating that the sensitivity is improved. The RMSE $/|k|$ is used to characterize the accuracy of the impedance method of stress measurement, and the statistical results are obtained as shown in Table I. It can be seen that the sensitivity of stress measurement after magnetization is 1.29× that before magnetization; magnetization makes the accuracy of stress measurement improve from 5.429 to 3.278 MPa for an almost constant impedance measurement error.

B. Measurement of Stress Distribution in Bent Steel

The impedance values Z after probe attachment were measured at 0.3, 0.5, 0.8, 1, 1.5, 2, 2.2, 2.5, and 2.7 m of the sandwich structure before and after magnetization. Curve fitting of stress values measured by FBGs using a sixth order polynomial function, and the results are shown in Fig. 9. Here are the results for W = 0 kg; others are given in Fig. S1 of the "Stress distribution measurement results of sandwich steel plates" in the Supplemental Material. It can be seen that after the sandwich structure is magnetized, the impedance distribution measured by the probe can well overlap the stress distribution measured by the FBGs under different loads, which proves that the magnetization can significantly improve the consistency of stress measurement with the electromagnetic impedance method. Before the sandwich structure is magnetized, the impedance distribution measured by the probe and the stress measured by the FBG has poor consistency.

The impedance-stress relationships at different measurement points of the sandwich structure were further analyzed quantitatively. Taking the center of the structure as the demarcation point, the impedance and stress measured at different measurement points of the left and right segments are fit, respectively. The measurement and fitting results before and after magnetization are obtained. The results are displayed in Fig. 10. Here are the results for W = 0 kg; others are given in Fig. S2 of the "Stress distribution measurement results of sandwich steel plates" in the Supplemental Material, and the important information in the figure is summarized in Table II. It can be seen that the fitting effect of the left and right segments before magnetization is very poor, the goodness-of-fit R^2 is lower than 0.85, and the slope k of the fit curves of the left and right segments differs greatly, indicating poor consistency; whereas the fitting effect of the left and right segments after magnetization is very good, the goodness-of-fit R^2 is higher than 0.9, and the difference in the slope k of the fit curves of the left and right segments is very small, indicating good consistency.

Tables III and IV present the residual RMSE and the absolute slope $|k|$ of the Z-σ fitting results, as well as the equivalent stress measurement error RMSE/$|k|$ with different loading weights before and after magnetization for comparison. It can be seen that the sensitivity of the plate stress measurement before magnetization is 0.009–0.022 Ω/MPa with an average of 0.014 Ω/MPa. The sensitivity of the stress measurement after magnetization was 0.031–0.048 Ω/MPa, with an average of 0.037 Ω/MPa. Magnetization increased the stress measurement sensitivity by 2.6. As the stress increases, the sensitivity decreases. This is due to the deformation of the steel plate caused by the application of weights. The air gap between the probe and the steel plate increases, resulting in an increase in magnetoresistance and a decrease in initial permeability, resulting in a decrease in sensitivity. To prove this conclusion, we conduct impedance change detection experiments corresponding to different air gap sizes and tensile experiments on a steel plate. The experimental process and results are given in the "Influence of air gap on stress measurement based on electromagnetic impedance method" of the Supplemental Material. The average RMSE/$|k|$ value of the measurement accuracy at different load states before magnetization was 50.699 MPa. The average RMSE/$|k|$ value of the measurement accuracy at different load states

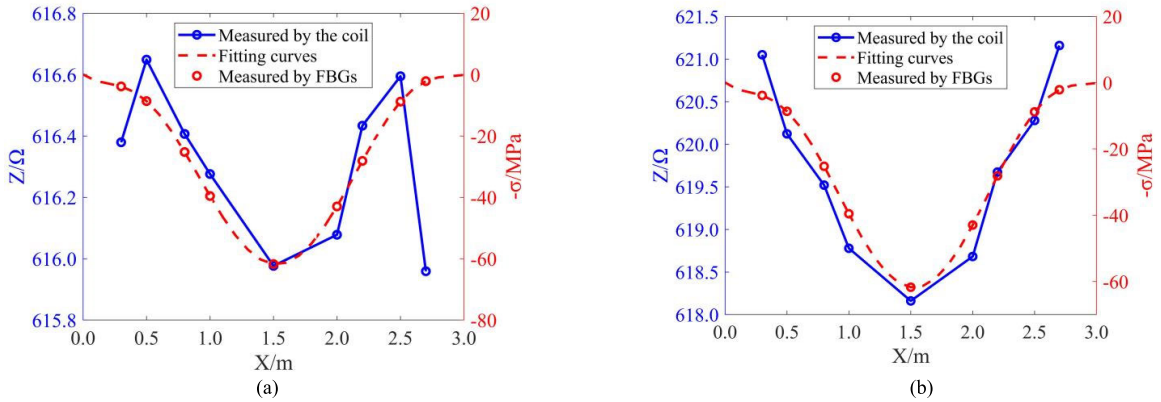

Fig. 9. Stress and impedance distribution measured at different locations with different loads before and after magnetization. (a) $W = 0$ kg, without magnetization. (b) $W = 0$ kg, with magnetization.

TABLE II

IMPEDANCE AND STRESS MEASUREMENT AND FITTING RESULTS IN THE LEFT AND RIGHT SEGMENT OF THE SANDWICH STRUCTURE UNDER DIFFERENT LOADS BEFORE AND AFTER MAGNETIZATION

W	Index	Without magnetization	With magnetization
0 kg	Left	$z = -0.022\sigma + 617.47, R^2 = 0.7615$	$z = -0.046\sigma + 620.81, R^2 = 0.9303$
	Right	$z = -0.011\sigma + 616.84, R^2 = 0.1437$	$z = -0.048\sigma + 620.98, R^2 = 0.9597$
1 kg	Left	$z = -0.021\sigma + 617.42, R^2 = 0.8009$	$z = -0.039\sigma + 620.72, R^2 = 0.9394$
	Right	$z = -0.011\sigma + 616.78, R^2 = 0.1720$	$z = -0.042\sigma + 620.98, R^2 = 0.9573$
2 kg	Left	$z = -0.017\sigma + 617.19, R^2 = 0.7140$	$z = -0.036\sigma + 620.70, R^2 = 0.9630$
	Right	$z = -0.011\sigma + 616.74, R^2 = 0.2210$	$z = -0.038\sigma + 620.85, R^2 = 0.9640$
3 kg	Left	$z = -0.016\sigma + 617.08, R^2 = 0.7828$	$z = -0.033\sigma + 620.52, R^2 = 0.9788$
	Right	$z = -0.011\sigma + 616.66, R^2 = 0.2574$	$z = -0.036\sigma + 620.85, R^2 = 0.9700$
4kg	Left	$z = -0.014\sigma + 616.81, R^2 = 0.7698$	$z = -0.031\sigma + 620.45, R^2 = 0.9854$
	Right	$z = -0.010\sigma + 616.56, R^2 = 0.2814$	$z = -0.033\sigma + 620.70R^2 = 0.9783$
5 kg	Left	$z = -0.012\sigma + 616.73, R^2 = 0.7577$	$z = -0.031\sigma + 620.48, R^2 = 0.9888$
	Right	$z = -0.009\sigma + 616.46, R^2 = 0.2556$	$z = -0.032\sigma + 620.66, R^2 = 0.9765$

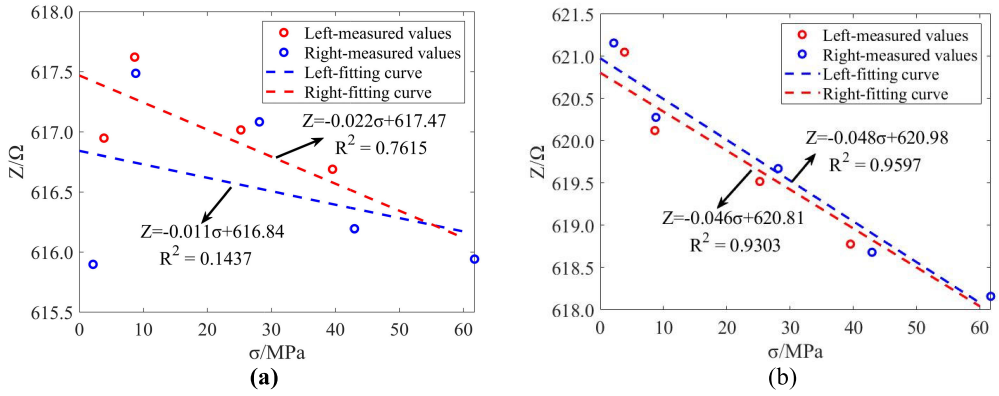

Fig. 10. Impedance and stress measurement and fitting results in the left and right segment of the sandwich structure under the load of $W = 0$ kg before and after magnetization. (a) Without magnetization. (b) With magnetization.

after magnetization is 7.078 MPa, which is 7.2× that before magnetization. It can be seen from the above results that magnetization can significantly improve the sensitivity and consistency of stress measurement when using the impedance method, and the stress distribution law of the sandwich structure can be successfully measured after the steel is magnetized. To analyze the validation of repeatability and hysteresis effects, experiments with different dates and different magnetization times are carried out. The results indicate that the impedance values measured after the same magnetization have a small difference and high repeatability. The results also indicate that there is a hysteresis phenomenon in the permeability. Hysteresis may reduce the repeatability of single-point stress measurement, such as single-point monitoring of the crane; however, when measuring the distribution of a long steel pipeline or rail, the hysteresis is not a problem. This is because the stress test results are compared at different places in regard to the current stress state rather than at different

TABLE III
COMPARISON OF STRESS MEASUREMENT PERFORMANCE OF SANDWICH STEEL PLATES UNDER DIFFERENT LOADS WITHOUT MAGNETIZATION

Index	W=0kg		W=1kg		W=2kg		W=3kg		W=4kg		W=5kg	
	Left	Right	Left	Right	Left	Right	Left	Right	Left	Right	Left	Right
$\|k\|$/(Ω/MPa)	0.022	0.011	0.021	0.011	0.017	0.011	0.016	0.011	0.014	0.010	0.012	0.009
RMSE/Ω	0.344	0.771	0.345	0.810	0.416	0.822	0.370	0.822	0.374	0.825	0.384	0.849
RMSE/$\|k\|$ /(MPa)	15.636	70.091	16.429	73.636	24.471	74.727	23.125	74.727	26.714	82.500	32.000	94.333

TABLE IV
COMPARISON OF STRESS SENSITIVITY AND MEASUREMENT PERFORMANCE OF SANDWICH STEEL PLATES UNDER DIFFERENT LOADS WITH MAGNETIZATION

Index	W=0kg		W=1kg		W=2kg		W=3kg		W=4kg		W=5kg	
	Left	Right	Left	Right	Left	Right	Left	Right	Left	Right	Left	Right
$\|k\|$/(Ω/MPa)	0.046	0.048	0.039	0.042	0.036	0.038	0.033	0.036	0.031	0.033	0.031	0.032
RMSE/Ω	0.344	0.279	0.332	0.305	0.278	0.189	0.250	0.271	0.189	0.250	0.179	0.276
RMSE/$\|k\|$ /(MPa)	7.478	5.813	8.513	7.262	7.722	4.973	7.576	7.528	6.097	7.576	5.774	8.625

times far apart. In addition, only one magnetization is required during the moving and distribution measurement, so the lower reproducibility at different dates and with different magnetization does not affect the measurement of the plate stress distribution. The detailed experimental process and results are given in the "Repeatability and hysteresis experiments" of the Supplemental Material.

V. CONCLUSION

In this article, a distributed stress measurement method for ferromagnetic steel plates based on active strong magnetization and magnetoelastic effect is proposed and the following conclusions can be drawn.

1) Via numerical calculation based on the J-A model, it is clarified that strong remnant magnetization can improve the sensitivity and consistency of the stress measurement of ferromagnetic materials by lowering the material planning constant a, lowering the initial permeability μ_{r0}, and increasing the magnetic domain coupling coefficient α, and homogenizing these parameters.
2) The principle of stress measurement based on the electromagnetic impedance method is analyzed, and the negative linear expression of the impedance with respect to stress is obtained. The correctness of the impedance expression was verified by experiments. It is demonstrated that an increase in excitation frequency can increase the impedance-stress sensitivity. When the excitation frequency is 30 kHz, and the elastic stress variation range is 0–130 MPa, the stress measurement sensitivity after magnetization is 1.29× that before magnetization, and the magnetization makes the single-point stress measurement accuracy improve from 5.429 to 3.278 MPa.
3) The impedance value of the probe can accurately reflect the state of stress distribution after the steel plate is magnetized. For the sandwich structure with the upper and lower steel plates of Q235 in dimensions of 3000 × 120 × 3 mm and the neutral layer of PA6 in dimensions of 3000 × 120 × 20 mm, before magnetization, the sensitivity of the distributed stress measurement is 0.014 Ω/MPa in average, and the accuracy is 50.699 MPa in average under different loads; after magnetization, the average sensitivity of distributed stress measurement is 0.037 Ω/MPa and the average accuracy is 7.078 MPa. After magnetization, the sensitivity of stress measurement is increased by 2.6×, and the accuracy is increased by 7.2×. It can, therefore, be concluded that magnetization can significantly improve the sensitivity and consistency of stress measurement with the electromagnetic impedance method.

REFERENCES

[1] A. Díaz, I. I. Cuesta, J. M. Alegre, A. M. P. de Jesus, and J. M. Manso, "Residual stresses in cold-formed steel members: Review of measurement methods and numerical modelling," *Thin-Walled Struct.*, vol. 159, Feb. 2021, Art. no. 107335.
[2] Z. Zeng, C. Zhao, X. Huang, J. Li, and S. Chen, "Non-invasive pressure measurement based on magneto-mechanical effects," *Meas. Sci. Technol.*, vol. 29, no. 9, Aug. 2018, Art. no. 095106.
[3] L. Wei, S. Su, W. Wang, and M. Yan, "Characterization of buckling of a steel box girder under bending using parameter of magnetic memory," *J. Vib. Shock*, vol. 41, no. 16, pp. 142–148, Aug. 2022.
[4] T. Liu, B. Liu, G. Feng, Z. Lian, and L. Yang, "Quantization of pipeline magnetic flux leakage detection signal under load," *Chin. J. Sci. Instrum.*, vol. 43, no. 1, pp. 262–273, Jan. 2022.
[5] Z. Zhang, N. He, B. He, B. Xu, and Y. Jiang, "A new method for structural stress measurement based on distributed optical fiber sensing technology," *Instrument*, vol. 41, no. 9, pp. 45–55, Mar. 2020.
[6] N. Subedi, T. Obara, and S. Kono, "Noncompact and slender concrete-filled steel tubes under axial compression: Finite-element modeling and evaluation of stress-strain models for fiber-based analysis," *J. Constructional Steel Res.*, vol. 196, Sep. 2022, Art. no. 107353.
[7] Z. Li, J. He, J. Teng, Q. Huang, and Y. Wang, "Absolute stress measurement of structural steel members with ultrasonic shear-wave spectral analysis method," *Struct. Health Monitor.*, vol. 18, no. 1, pp. 216–231, Jan. 2019.

[8] J. He, Z. Li, J. Teng, and Y. Wang, "Comparison of the Lcr wave TOF and shear-wave spectrum methods for the uniaxial absolute stress evaluation of steel members," *Struct. Control Health Monitor.*, vol. 26, no. 6, p. e2348, Mar. 2019.
[9] Y. Xu et al., "Research progress on magnetic memory nondestructive testing," *J. Magn. Magn. Mater.*, vol. 565, Jan. 2023, Art. no. 170245.
[10] S. Ren and X. Ren, "Studies on laws of stress-magnetization based on magnetic memory testing technique," *J. Magn. Magn. Mater.*, vol. 449, pp. 165–171, Mar. 2018.
[11] G. Qiu, Y. Cai, and Z. Li, "Multiscale investigation of magnetic field distortion on surface of ferromagnetic materials caused by stress concentration for metal magnetic memory method," *Comput. Mater. Sci.*, vol. 209, Jun. 2022, Art. no. 111353.
[12] Z. Li, S. Dixon, P. Cawley, R. Jarvis, P. B. Nagy, and S. Cabeza, "Experimental studies of the magneto-mechanical memory (MMM) technique using permanently installed magnetic sensor arrays," *NDT E Int.*, vol. 92, pp. 136–148, Dec. 2017.
[13] H. Li, C. Zhao, F. Zhang, Z. Hu, and L. Ding, "An experimental study of relationship between stress and excitation magnetic field," *IEEE Trans. Instrum. Meas.*, vol. 72, pp. 1–9, 2023.
[14] G. C. Hakan, "Review of residual stress measurement by magnetic Barkhausen noise technique," *Mater. Perform. Charact.*, vol. 7, no. 4, pp. 504–526, May 2018.
[15] Y. Liu, Q. Liu, R. Gao, B. Gao, and G. Tian, "Stress measurement of ferromagnetic materials using hybrid magnetic sensing," *IEEE Trans. Instrum. Meas.*, vol. 72, pp. 1–13, 2023.
[16] F. Qiu, M. Jovicevic-Klug, G. Tian, G. Wu, and J. McCord, "Correlation of magnetic field and stress-induced magnetic domain reorientation with Barkhausen noise," *J. Magn. Magn. Mater.*, vol. 523, Apr. 2021, Art. no. 167588.
[17] S. Doi, T. Aoki, K. Okazaki, Y. Takahashi, and K. Fujiwara, "Study of computation method of iron loss considering magnetic anisotropy by processing residual stress," *Elect. Eng. Jpn.*, vol. 204, no. 1, pp. 29–39, 2018.
[18] F. Zhang, H. Li, C. Shi, and R. Jia, "Stress-induced magnetic anisotropy model under unidirectional tension," *IEEE Access*, vol. 8, pp. 4769–4774, 2020.
[19] W. Xin, L. Liang, K. Ding, Y. Zhao, and H. Wang, "Study on the magnetic measurement theory and method of residual stress for ferromagnetic components based on magnetic anisotropy," *Chin. J. Sci. Instrum.*, vol. 41, no. 11, pp. 137–146, Nov. 2020.
[20] Z. Su, J. Xin, Q. Zhang, J. Chen, and Y. Guo, "Transient force-magnetic coupling simulation research on pipeline stress concentration," *J. Phys., Conf.*, vol. 2383, no. 1, Dec. 2022, Art. no. 012151.
[21] K. Tong, J. Zhou, R. Zhao, H. Ying, and S. Zhang, "Quantitative measurement of stress in steel bars under repetitive tensile load based on force-magnetic coupling effect," *Measurement*, vol. 202, Oct. 2022, Art. no. 111820.
[22] D. C. Jiles and D. L. Atherton, "Theory of ferromagnetic hysteresis," *J. Magn. Magn. Mater.*, vol. 61, nos. 1–2, pp. 48–60, Sep. 1986.
[23] D. C. Jiles and M. K. Devine, "Recent developments in modeling of the stress derivative of magnetization in ferromagnetic materials," *J. Appl. Phys.*, vol. 76, no. 10, pp. 7015–7016, Nov. 1994.
[24] D. C. Jiles and M. K. Devine, "The law of approach as a means of modelling the magnetomechanical effect," *J. Magn. Magn. Mater.*, vol. 140, pp. 1881–1882, Feb. 1995.
[25] S. Wang, W. Wang, S. Su, and S. Zhang, "A magneto mechanical model of the relationship between relative permeability change and stress of ferromagnetic materials," *J. Xi'an Univ. Sci. Technol.*, vol. 25, no. 3, pp. 288–291 and 305, Jul. 2005.
[26] L. Shan et al., "Remanent magnetization of steel plates after being magnetized by moving magnets," *J. Magn. Magn. Mater.*, vol. 578, Jul. 2023, Art. no. 170818.

Hongbin Zhang was born in Cangzhou, Hebei, China, in 2000. He received the B.E. degree in measurement and control technology and instrument from the Hebei University of Technology, Tianjin, China, in 2022. He is currently pursuing the M.E. degree with Tianjin University, Tianjin, under the guidance of Associate Professor Xinjing Huang.

His research interests include pipeline stress measurement, signal feature extraction, and the application of magnetic sensors.

Yuan Wang was born in Handan, Hebei, China, in 1998. He received the B.E. degree in measurement and control technology and instrument from the Hebei University of Technology, Tianjin, China, in 2020, and the M.E. degree from Tianjin University, Tianjin, in 2023, where he is currently pursuing the Ph.D. degree under the guidance of Associate Professor Xinjing Huang.

His research interests include magnetic field measurement, signal processing, and pipeline leak detection.

Qian Chen was born in Fuzhou, Jiangxi, China, in 1998. He received the B.E. degree in opto-electronic information science and control from the Hefei University of Technology, Hefei, China, in 2016, and the M.E. degree from Tianjin University, Tianjin, China, in 2023.

His main interests include pipeline stress detection and pipeline safety warning.

Jinyu Ma received the B.E. and M.E. degrees in instrument science and technology from the Shandong University of Science and Technology, Qingdao, China, in 2010 and 2012, respectively, and the Ph.D. degree in instrument science and technology from Tianjin University, Tianjin, China, in 2016.

In 2016, she joined the Sensor and Electronic Testing Laboratory, Tianjin University, as a Lecturer and an Engineer, where she also works with the State Key Laboratory of Precision Measurement Technology and Instruments. Her research topics mainly cover electric sensing and measurement, precision measuring circuits, and measurement and control based on embedded systems.

Jian Li received the B.E., M.E., and Ph.D. degrees in instrument science and technology from Tianjin University, Tianjin, China, in 1994, 1997, and 2000, respectively.

He is currently a Full Professor with the School of Precision Instrument and Opto-Electronics Engineering, Tianjin University, where he also works with the State Key Laboratory of Precision Measurement Technology and Instruments. His research topics mainly cover test signal processing, weak signal detection, and target detection technology and instruments.

Xinjing Huang received the B.E. and Ph.D. degrees in instrument science and technology from Tianjin University, Tianjin, China, in 2010 and 2016, respectively.

He is currently an Associate Professor with the School of Precision Instrument and Opto-Electronics Engineering, Tianjin University, where he also works with the State Key Laboratory of Precision Measurement Technology and Instruments. His research topics mainly cover structural health inspection and/or monitoring technology and intelligent perception electronic systems with acoustic and/or magnetic methods.